

**TIDAL DISRUPTION OF RUBBLE-PILE BODIES: INFLUENCES OF INTERNAL STRUCTURE AND MATERIAL FRICTION.** Y. Zhang<sup>1</sup> and P. Michel<sup>1</sup>, <sup>1</sup>Université Côte d'Azur, Observatoire de la Côte d'Azur, CNRS, Laboratoire Lagrange, Nice, France (yun.zhang@oca.eu).

**Introduction:** The chaotic dynamical evolution of small bodies in our Solar System sometimes leads some of them to experience very close encounters with planets that can either cause surface motion, modify their shapes or even disrupt them [1, 2]. Such tidal effects require a good understanding as they may be responsible for some of the observed characteristics of rubble-pile small bodies and therefore may give important clues on their history and structures. The outcomes of tidal processes highly depend on the initial conditions of those encounters as well as on the internal structure and other characteristics of the involved bodies [3].

Dynamical modeling is a powerful tool to reveal the details of tidal processes. Previous studies on this topic represented the rubble-pile objects as granular aggregates made of identical spheres in a hexagonal-close-packed (HCP) configuration [4, 5], which does not represent well the nature of rubble-pile bodies made of randomly distributed particles. Here we investigate the tide-induced surface and internal modifications of self-gravitating rubble piles using a Soft-Sphere Discrete Element Method (SSDEM). The effects of initial configuration of rubble-pile models and interparticle friction are numerically explored.

**Methodology:** We use a high-efficiency SSDEM code, *pkdgrav*, to simulate the dynamical behaviors of self-gravitating rubble piles during close planetary encounters. A granular physics model including 4 dissipation/friction components in the normal, tangential, rolling, and twisting directions is applied for computing particle contact forces [6,7]. These quantities determine the magnitude of the material shear strength.

**Simulation setup:** We physically model the dynamical processes acting on rubble piles during an Earth flyby. The rubble-pile object is modelled as a spherical granular assembly consisting of  $\sim 10,000$  identical spherical particles. We explore two possible configurations in this study: an HCP configuration and a random close packing (RCP) configuration. The initial bulk density is set to  $\sim 2.47$  g/cc and radius is set to 1 km. Prior to the encounter, the spherical progenitor has a prograde rotation with a spin period of 4.3 h. Three material friction angles ranging from  $18^\circ$  to  $32^\circ$  are tested for the RCP model. The simulated rubble pile approaches the Earth on different hyperbolic orbits, which can be defined by its encounter velocity at infinity,  $V_\infty$ , and its perigee distance,  $q$ . The theoretical

tidal failure limit distance of the Earth ( $M_E = 5.97 \times 10^{24}$  kg,  $R_E = 6378$  km),  $d_{\text{limit}}$ , for a cohesionless rubble pile with a friction angle of  $20^\circ$  and a bulk density of 2.47 g/cc is about  $2.4R_E$  [3]. Therefore, the perigee distance is set to range from  $2.5R_E$  to  $1.1R_E$  and the velocity at infinity is set to range from 0 km/s (parabolic orbit) to 20 km/s in our tests. The tested rubble pile is taken to start  $15d_{\text{limit}}$  from Earth, which is large enough to ensure that Earth's perturbations are negligible at the outset. Each run is terminated when all the tide-induced fragments (or the reshaping rubble pile) have settle down to stable states.

**Results:** The simulation results show a similar behavior of the rubble-pile body in response to tidal forces as found in previous studies [2]. Figure 1 presents the mass of the largest remnant relative to the initial body for the RCP model with a variety of friction angles for different close approach distances  $q$  and encounter speeds  $V_\infty$ . Due to the intrinsic material shear strength and the short flyby time, the rubble-pile object can only be tidally disrupted at a distance notably lower than the theoretical tidal failure limit distance (e.g., mass loss occurs when  $q < 1.9R_E$  for the lowest friction case). For weak encounters, where the perigee distance is close to the tidal failure limit distance, the rubble pile is slightly distorted to a prolate shape when passing by the planet. The distortion of the object becomes more severe with a smaller perigee distance. When the perigee distance is close to  $1.4R_E$ , the rubble pile is spun up, heavily distorted and then disrupted by Earth's tides. Since the tidal forces are dramatically increasing with a decreasing perigee distance, the progenitor is subject to more brutal disruption and is split into larger amounts of fragments for a closer orbit.

Figure 1 clearly shows the trend that rubble piles are harder to be tidally disrupted with a higher friction angle. The surface friction and rotational resistance between the constituent particles impede their relative movements, and the vibrations of particles due to the tidal encounter can be quickly damped out when the body flies away from the Earth. The friction resistance also affects the reshaping path of the rubble pile. Although the tidal forces pull and accelerate the rubble pile to exceed its spin limit, the subsequent reshaping process rapidly slows it down. The largest remnants often have a slower spin rate than the initial value and are subject to stresses that tend to make the shape rounder and spin faster. With increasing friction, the

remnants can keep an elongated stable shape at a lower spin rate.

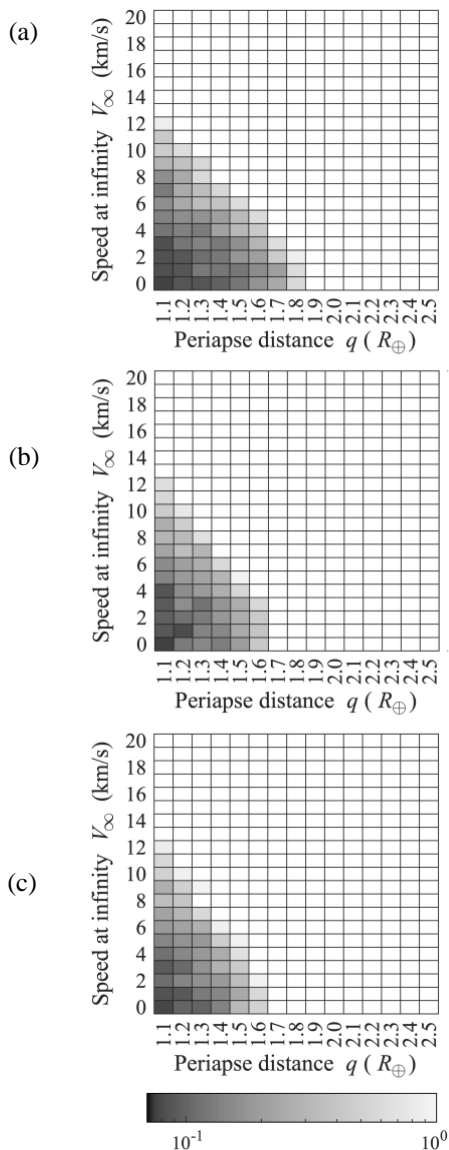


**Figure 1** The mass ratio of the largest remnant to the original mass of the rubble-pile as a function of  $V_\infty$  and  $q$  for the RCP model with different friction angles, where (a)  $\phi = 18^\circ$ , (b)  $\phi = 27^\circ$ , (c)  $\phi = 32^\circ$ .

Figure 2 shows the largest remnants' masses for the case of HCP configuration and compares our SSDEM results with the results using hard-sphere discrete element method (HSDEM) with the same encounter scenarios by previous study [8]. Owing to the geometrical effects of particle interlocking, the HCP configuration can resist much higher shear stress than an RCP model of the same material. Mass loss is slightly smaller than the case of the RCP model (see Figure 1(a)). Comparing the mass loss behaviors, the rubble pile using HSDEM is much easier to be tidally disrupted

than using SSDEM. This is because the surface contact is not physically modelled in HSDEM. Without properly considering the surface friction, bouncing between particles can lead to disruption during a close encounter.

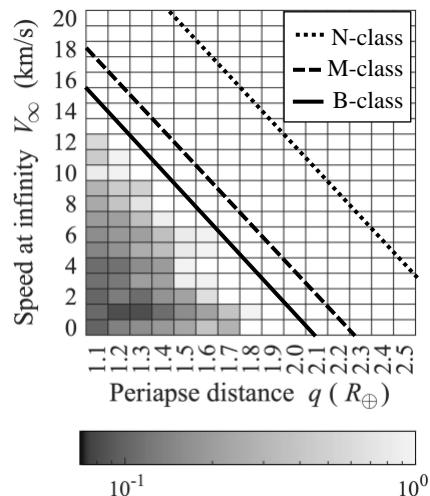


**Figure 2** The same as Figure 1, but for the HCP model with similar material parameters than those of the minimum friction case of RCP where  $\phi = 18^\circ$ . The three lines plotted on the top-left panel indicate the tidal disruption mass loss outcomes of previous simulations using HSDEM [8], where above the N-class line the progenitor has no mass loss, below the M-class line more than 10% of the progenitor's original mass is lost, below the B-class line the mass loss is larger than 50%.

**Conclusion:** We have run a suite of tidal disruption simulations to reveal the effect of internal configuration and friction on the reshaping and disruption behaviors of rubble-pile bodies using an SSDEM code and compared our results with previous simulations that used more simplistic particle interactions. We find that friction can decrease the mass loss behaviors and dramatically change the dynamics of the disruption.

**Acknowledgments:** Y. Z. acknowledges funding from the Université Côte d'Azur "Individual grants for young researchers" program of IDEX JEDI. P. M. acknowledges support from CNES and from the Acad. 2 and 3 of Univ. Côte d'Azur IDEX JEDI.

#### References:

- [1] Bottke W. F. et al. (1999) *AJ*, 117, 1921–1928.
- [2] Richardson D. C. et al. (1998) *Icar*, 137, 47–76. [3] Holsapple K. A. & Michel P. (2008) *Icar*, 193, 283–301.
- [4] Walsh K. J. & Richardson D. C. (2008) *Icar*, 193, 553–566. [5] DeMartini J. V. et al. (2019) *Icar*, 328, 93–103. [6] Schwartz S. R. et al. (2012) *Granular Matter*, 14, 363–380. [7] Zhang Y. et al. (2017) *Icar*, 294, 98.
- [8] Schunová E. et al. (2014) *Icar*, 238, 156–169.